IEEE Photonics Journal
An IEEE Photonics Society Publication

Open Access

Digital Phase Noise Compensation for DSCM-Based Superchannel Transmission System With Quantum Dot Passive Mode-Locked Laser

Volume 10, Number 4, August 2018

Govind Vedala, *Student Member, IEEE*
Maurice O' Sullivan, *Senior Member, IEEE*
Rongqing Hui, *Senior Member, IEEE*

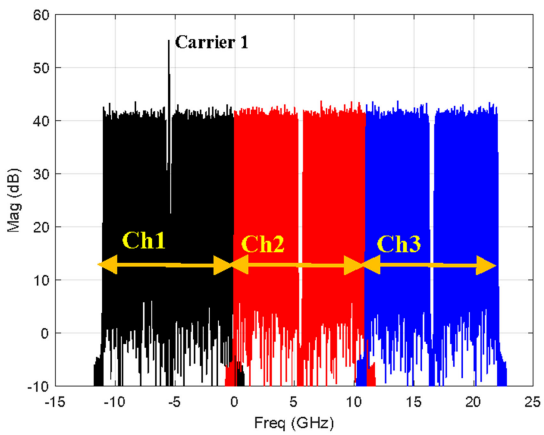

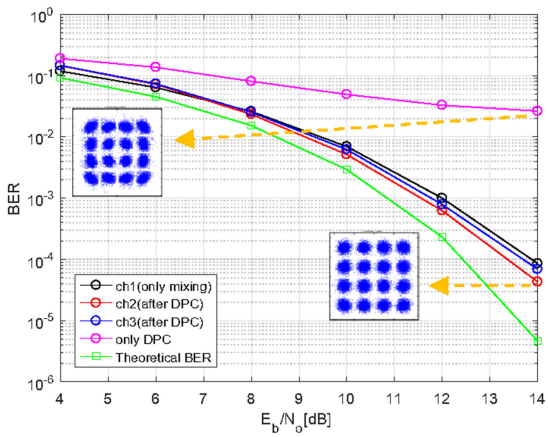

DOI: 10.1109/JPHOT.2018.2841660
1943-0655 © 2018 IEEE

IEEE photonics SOCIETY

IEEE

Digital Phase Noise Compensation for DSCM-Based Superchannel Transmission System With Quantum Dot Passive Mode-Locked Laser

Govind Vedala,[1] ***Student Member, IEEE***,
Maurice O' Sullivan,[2] ***Senior Member, IEEE***,
and Rongqing Hui,[1] ***Senior Member, IEEE***

[1]Department of Electrical Engineering and Computer Science, University of Kansas, Lawrence, KS 66045 USA
[2]Ciena Corp., Nepean, ON, K2K 0L1, Canada

DOI:10.1109/JPHOT.2018.2841660
1943-0655 © 2018 IEEE. Translations and content mining are permitted for academic research only. Personal use is permitted, but republication/redistribution requires IEEE permission. See http://www.ieee.org/publications_standards/publications/rights/index.html for more information.

Manuscript received March 29, 2018; revised May 12, 2018; accepted May 24, 2018. Date of publication May 28, 2018; date of current version June 26, 2018. This work was supported in part by US National Science Foundation under Grant 1409853. Corresponding author: Govind Vedala (e-mail: govind.vedala@ku.edu).

Abstract: We propose a simplified digital phase noise compensation technique for a Nyquist pulse-shaped digital subcarrier multiplexed (DSCM) coherent optical transmission system, employing an optical frequency comb based on Quantum dot passive mode-locked laser (QD-PMLL). Our results show that the impact of dominant common mode phase noise can be efficiently compensated at the receiver by digitally mixing the data sideband with the complex conjugate of the residual carrier component. This digital mixing technique resulted in better bit error rate performance compared to the conventional mth power Viterbi–Viterbi algorithm for QPSK and blind phase noise compensation for 16-quadratic-amplitude modulation formats, especially in the presence of large phase noise. To this end, exploiting the mutual coherence between the mode-locked comb lines of QD-PMLL, we numerically demonstrate its potential applicability as a transmission source for coherent optical superchannel transmission.

Index Terms: Quantum dots, Nyquist subcarrier, superchannel, DSCM, phase noise, DSP, digital mixing.

1. Introduction

Coherent optical frequency combs, which produce mutually coherent spectral lines, are ideal light sources for coherent optical WDM (CoWDM) and superchannel fiber-optic transmission systems with coherent receivers. Mutual phase coherence among spectral lines has been utilized to control inter-channel crosstalk in CoWDM [1] and compensate carrier phase noise using joint carrier phase estimation in superchannel transmission systems [2]. These coherent frequency combs can be generated using dispersive parametric mixing in highly nonlinear fibers [3], and carrier-suppressed single sideband modulation in fiber-optic re-circulating loops [4] to name a few. Passive mode locked semiconductor diode lasers with simple structure and miniature footprint, are of interest to the lightwave communications community as potential sources for Tb/s data transmission [5], [6]. Quantum dash and quantum dot semiconductor materials have been used in comb lasers.

Owing to inhomogeneous broadening, mode competition between spectral modes is reduced for these materials. In addition to providing wide gain bandwidth with relatively flat spectral profile, a diode laser based optical frequency comb can be integrated with other photonic components such as splitters, combiners and electro-optic modulators based on planar lightwave circuits (PLC) [7]. Use of passive mode locked diode lasers for short reach applications such as communication among datacenters has been reported [8], wherein Tb/s data rates were achieved using intensity modulation and direct detection. Along with the afore mentioned properties, diode laser based PM-LLs typically have broader spectral linewidth compared to other coherent optical frequency combs. Spontaneous emission, linewidth enhancement factor, and timing jitter are dominant contributions to phase noise which can amount to a multi-MHz spectral linewidth that limits the application of such devices in coherent optical systems. In comparison, a direct detection receiver is sensitive only to optical signal amplitude and is immune to such phase noise, (assuming fiber chromatic dispersion is compensated optically or digitally). Thus QD-PMLLs are more readily compatible with direct detection applications such as found in data centers. In a direct detection receiver based on a single APD or PIN photodiode, mode partition noise from the QD-PMLL affects system performance especially for higher order modulation formats [8]. This is not a major concern for coherent receivers, as balanced detection suppresses the intensity fluctuations. However, when using complex optical field modulation with coherent detection, efficient digital signal processing (DSP) algorithms should be adopted in the receiver to estimate and compensate the phase noise on data symbols. The broad spectral linewidth of QD-PMLL poses a tough challenge for digital phase noise compensation at the receiver for the reasons stated below.

The impact of phase noise and its compensation depends on linewidth symbol-time product which has an upper bound that varies with different modulation formats as demonstrated in [9], [10]. This sets the performance limit for feedforward carrier phase recovery techniques employing mth power Viterbi-Viterbi algorithm for M- PSK or blind phase search algorithm for M-QAM signals. For example, as linewidth symbol-time product exceeds 8×10^{-5} for QPSK and 1.4×10^{-4} for 16-QAM, the above-mentioned carrier phase recovery techniques may fail to track the phase noise.

Self-homodyne coherent system was recently demonstrated [11] to overcome the impact of large phase noise. Spectral lines were modulated on one polarization and unmodulated spectral lines on the orthogonal polarization to achieve self-homodyne detection. The same research group also demonstrated the use of analog electronics and optics for removing the common mode phase noise across comb lines before data modulation in the transmitter [12].

In this work, we demonstrate for the first time, a simple and effective digital mixing technique in the context of Nyquist pulse shaped DSCM system employing QD-PMLL as the source for optical carriers. This allows eliminating the contribution of common mode phase noise among different optical carriers of a QD-PMLL. DSCM enables spectrally efficient transmission with flexible baud rates and modulation formats on each subcarrier. Subcarrier multiplexing is also tolerant to Kerr effect induced nonlinearities, extending the transmission reach [13], [14]. The proposed digital mixing technique is also valid for single carrier systems. However, as systems with multiple low baud rate subcarriers are more susceptible to the impact of optical phase noise compared to high baud rate single carrier systems (phase noise variance within a symbol is inversely proportional to baud rate), the effectiveness of the proposed technique is validated in the context of DSCM system which has the most stringent requirement on laser phase noise. Note that a similar approach of digital mixing has been previously proposed in FFT based OFDM transmission system [15] adopting an external cavity laser as the transmission source. As we shall see in the later sections, application of digital mixing in the context of optical carriers generated from QD-PMLL has an additional benefit compared to optical carriers generated from multiple independent laser sources. This is attributed to the mutual coherence among the comb lines from QD-PMLL [16] which can be exploited to design an efficient optical superchannel transmission system [3], [17] using digital mixing in the receiver DSP. We use the term “Tributary” to refer to data channels in the context of a superchannel. If the optical carriers are uncorrelated, each tributary of the superchannel should have an unsuppressed carrier to enable digital mixing at the receiver. This penalizes all the tributaries in terms of required SNR to achieve a given BER. However, mutual coherence between the comb lines enables us to

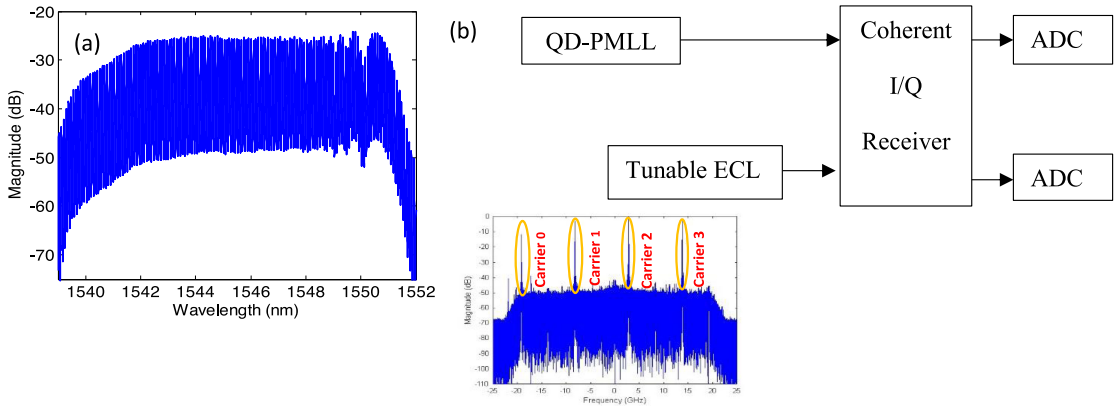

Fig. 1. (a). QD-PMLL optical spectrum, (b) Experimental setup for phase noise evaluation using optical heterodyne technique. Inset shows the spectrum of the four comb lines near 1542 nm obtained after optical heterodyning with an ECL.

suppress carriers in all but one tributary, restricting the SNR penalty to that tributary. To validate digital mixing technique in a superchannel based optical transmission system using semiconductor laser-based frequency comb as the light source, we used the complex optical waveform recorded from a QD-PMLL obtained through optical heterodyne measurement by mixing with a narrow linewidth external cavity laser (ECL) in a coherent receiver. In the frequency domain, this complex optical waveform has several discrete spectral comb lines. Three such spectral lines (in a sequence) are selected and modulated with Nyquist pulse shaped DSCM data in the digital domain to evaluate the performance of phase noise compensation algorithms. Digital mixing technique was compared with conventional feedforward carrier recovery algorithms namely, mth power Viterbi-Viterbi [18] and blind phase search algorithm [9], using bit error rate (BER) as the performance metric. The carrier to sideband power ratio (CSPR) defined as the ratio of the power in optical carrier to that in the data sidebands was found to play a vital role when using the digital mixing technique, and we find that there is an optimal CSPR value which minimizes the error probability.

2. Phase Noise Characterization of QD-PMLL and Its Mitigation Using Digital Mixing

A single section InAs/InP QD-PMLL was used as a laser source for evaluating the effectiveness of phase noise mitigation using digital mixing. Based on the measured complex optical field waveforms from this QD-PMLL, optical system performance and algorithms for digital phase noise compensation were evaluated by numerically creating Nyquist pulse shaped DSCM systems adopting different modulation formats. Fig. 1(a) shows the optical spectrum of comb lines from QD-PMLL measured by an optical spectrum analyzer with 0.01 nm spectral resolution. The QD-PMLL was driven at an injection current of 410 mA with an average output power from the fiber pigtail of approximately 9 mW. It has about 100 mutually coherent spectral lines within a 10 nm bandwidth (1540 nm to 1550 nm). The spacing between comb lines is approximately 11 GHz determined by the free-spectral range of the Fabry-Perot laser structure. Fig. 1(b) shows the block diagram of coherent heterodyne detection using a tunable ECL with $<$100 kHz spectral linewidth as the local oscillator (LO) in an in-phase/quadrature (I/Q) coherent optical receiver. The in-phase and the quadrature components of the frequency comb's optical field are captured by two photodiodes and digitized by a two-channel real time digital oscilloscope at a sampling rate of 50 Gsps corresponding to an acquisition time of 20 μs. The digitized in-phase and quadrature waveforms were used to reconstruct the complex optical field of the comb lines in the RF domain. Equations (1) and (2) respectively,

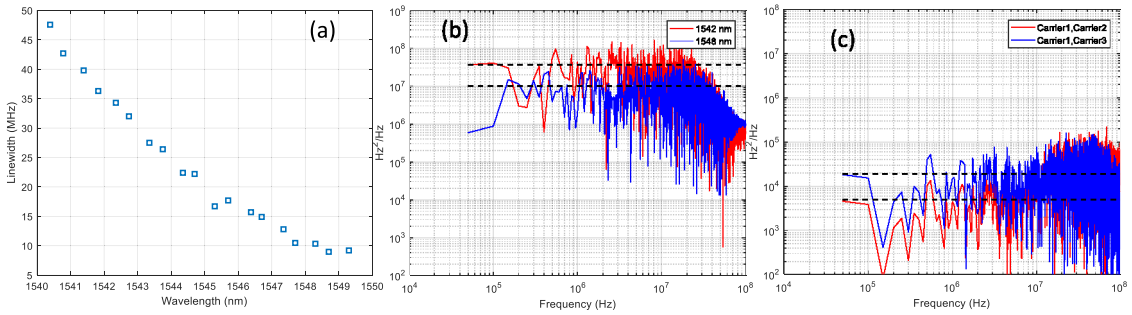

Fig. 2. (a) Optical linewidth as a function of wavelength obtained from the setup shown in Fig. 1. (b) the FM noise spectrum of the comb line in the vicinity of 1542 nm and 1548 nm.(c) FM noise spectrum of differential phase noise between carrier 1 and carrier 2 (red); carrier 1 and carrier 3(blue).

represent the complex optical field of QD-PMLL's frequency comb and the ECL.

$$E(t) = \sum_{n=1}^{N} E_n e^{j(\omega_n t + \theta_n(t))} \tag{1}$$

$$E_{LO}(t) = E_{lo} e^{j(\omega_{lo} t + \phi(t))} \tag{2}$$

where, E_n, ω_n, $\theta_n(t)$ correspond to the field amplitude, angular frequency, and phase noise of the nth spectral line of the QD-PMLL, respectively, and E_{lo}, ω_{lo}, $\phi(t)$ represent the field amplitude, angular frequency, and phase noise of the ECL. The contribution of $\phi(t)$ to the estimated optical linewidth of comb lines is assumed to be small and can be neglected. The complex waveform obtained from coherent I/Q receiver can be represented as

$$I + jQ = \sum_{n=1}^{N} E_n E_{lo}^{*} e^{j((\omega_n - \omega_{lo})t + \theta_n(t))} \tag{3}$$

where I and Q represent the in-phase and quadrature components of the complex waveform. For a given LO wavelength ω_{lo}, and a receiver bandwidth of ~23GHz, we could simultaneously reconstruct the complex optical field containing four comb lines, namely, Carrier 0,1,2 and 3, as shown in the inset of Fig. 1. The optical linewidth of a given comb line is characterized as follows. Applying fast Fourier transform (FFT) on the digitized complex optical field, we obtain the magnitude spectrum as shown in the inset of Fig. 1. A brick wall filter shaped by Hann window is used to extract one of the four comb lines whose complex field is represented by Equation (4) with $n = 1, 2, 3, 4$ representing the line index. For each selected spectral line, phase noise evolution as a function of time is determined from Equation (5) where $\theta(t)$ is equal to $\theta_n(t)$. The linewidth $\Delta\upsilon$ can be computed from Equations (6) and (7) by determining the phase noise power spectral density $S_\theta(f)$ and FM noise power spectral density $S_F(f)$. More specifically, an estimate of the linewidth is obtained by computing the average of frequency noise power spectral density given by Equation (7) over the given frequency range 60 kHz to 100 MHz.

$$I_{line} + jQ_{line} = E_{line} = E_n E_{lo}^{*} e^{j((\omega_n - \omega_{lo})t + \theta_n(t))} \tag{4}$$

$$\theta(t) = a\tan\left\{\frac{Q_{line}}{I_{line}}\right\} \tag{5}$$

$$S_F(f) = f^2 S_\theta(f) \tag{6}$$

$$\Delta\upsilon = 2\pi S_F(f) \tag{7}$$

Fig. 2(a) shows the measured optical linewidth as the function of wavelength which was obtained by varying the wavelength of LO in the coherent receiver. The FM noise spectra of comb lines in the vicinity of 1542 nm and 1548 nm are shown in Fig. 2(b). From Fig. 2(a) we observe that the optical linewidth steadily decreases towards the longer wavelengths with 37 MHz at 1542 nm and 10 MHz at 1548 nm. With respect to Equation (1), mode locking condition of comb lines ensures that

$$\theta_{\mathrm{n}}(\mathrm{t}) = \theta_{\mathrm{n}-1}(\mathrm{t}) + \delta\theta(\mathrm{t}) \tag{8}$$

$$\omega_{\mathrm{n}}(\mathrm{t}) = \omega_{\mathrm{n}-1}(\mathrm{t}) + \omega_{\mathrm{r}} \tag{9}$$

where $\delta\theta$(t) is the difference of phase noise between two adjacent spectral lines referred to as differential phase noise, ω_{r} is the angular repetition frequency. The phase noise of the n^{th} spectral line θ_{n}(t), can be decomposed into a summation, consisting of a common mode phase noise, common to all spectral lines and exclusive to the reference spectral line, as well as a differential phase noise relative to the reference spectral line [19].

$$\theta_{\mathrm{n}}(\mathrm{t}) = \theta_{\mathrm{c}}(\mathrm{t}) + \Delta\theta_{\mathrm{c,n}}(\mathrm{t}) = \theta_{\mathrm{c}}(\mathrm{t}) + (\mathrm{n}-\mathrm{c})\,\delta\theta(\mathrm{t}) \tag{10}$$

Where, θ_{c}(t) is the common mode phase noise of cth spectral line, $\Delta\theta_{\mathrm{c,n}}$(t) is the phase noise difference between cth spectral line and nth spectral line. The common mode phase noise originates from spontaneous emission and is responsible for identical phase noise evolution of all the comb lines in a mode locked laser. In time domain, this translates to jitter free optical pulses. An ideal mode locking scenario is characterized by only common mode phase noise yielding perfectly coherent comb lines. However, practically, the optical pulses are acted upon by timing jitter resulting in differential phase noise between any two adjacent comb lines. With reference to the inset of Fig. 1, Fig. 2(c) shows the FM noise spectrum of the differential phase noise between the carrier 1 and carrier 2, (i.e., the adjacent comb lines) in the 1542 nm regime along with the FM noise spectrum of differential phase noise between carrier 1 and carrier 3 (i.e., every other comb line). From this figure, we can infer that the differential linewidth between adjacent comb lines is approximately 5 kHz indicating strong mode locking of comb lines and the differential linewidth between every other comb line is approximately 19 kHz [16]. Since, the dominant contribution to the linewidth comes from common mode phase noise, digitally mixing the complex conjugated optical field of any one comb line with the entire comb will cancel its contribution to the broad linewidth. Any residual non-zero linewidth after digital mixing is attributed to differential phase noise. A mathematical explanation is presented below. Consider Equation (1) which can be modified as

$$\mathrm{E}(\mathrm{t}) = \sum_{\mathrm{n}=1}^{\mathrm{N}} \mathrm{E_n} e^{\mathrm{j}(\omega_{\mathrm{n}}\mathrm{t}+\theta_{\mathrm{n}}(\mathrm{t}))} = \sum_{\mathrm{n}=1}^{\mathrm{N}} \mathrm{E_n} e^{\mathrm{j}(\omega_{\mathrm{n}}\mathrm{t}+\theta_{\mathrm{c}}(\mathrm{t})+(\mathrm{n}-\mathrm{c})\delta\theta(\mathrm{t}))} \tag{11}$$

Let n = c be the reference spectral line with phase θ_{c}(t). Its complex optical field is given as

$$\mathrm{E_c} e^{\mathrm{j}(\omega_{\mathrm{c}}\mathrm{t}+\theta_{\mathrm{c}}(\mathrm{t}))} \tag{12}$$

Mixing the complex conjugate of (12) with (11) yields (13)

$$\mathrm{E}'(\mathrm{t}) = \sum_{\mathrm{n}=1}^{\mathrm{N}} \mathrm{E_n} \mathrm{E_c^*} e^{\mathrm{j}((\omega_{\mathrm{n}}-\omega_{\mathrm{c}})\mathrm{t}+(\mathrm{n}-\mathrm{c})\delta\theta(\mathrm{t}))} \tag{13}$$

which is independent of common mode phase noise θ_{c}(t). This is indeed the principle behind digital mixing phase noise compensation technique proposed and demonstrated in this work.

3. Semi-Numerical Simulation, Results and Discussion

A schematic of the semi-numerical simulation of a transmission system employing digital mixing is shown in Fig. 3. The measurement and simulation parameters are tabulated in Table 1. Various steps involved in the semi-numerical simulation are outlined as follows. An ideal optical I/Q modulator

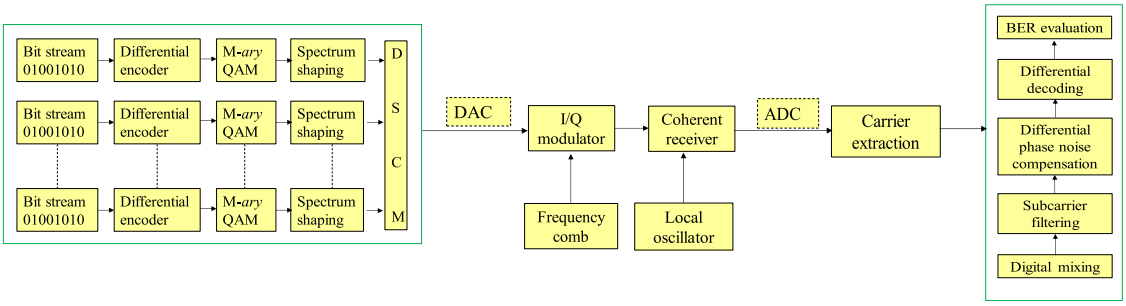

Fig. 3. Simulation setup with transmitter and receiver DSP stack.

TABLE I
MEASUREMENT AND SIMULATION PARAMETERS

Measurement Parameters	
Repetition frequency of comb lines	~11 GHz
Wavelengths of acquired comb lines	1542 nm, 1548 nm
Linewidth of acquired comb lines	37 MHz, 10 MHz
Differential linewidth of adjacent comb lines	~ 5 kHz
Tunable local oscillator linewidth	< 100 kHz
ADC analog bandwidth	23 GHz
ADC sampling rate	50 Gsps
Simulation Parameters	
No. of superchannel tributaries	3
No. of Nyquist subchannels per tributary	6
Nyquist roll-off factor	0
Nyquist subchannel bandwidth	1.75 GHz
Net superchannel bandwidth	31.5 GHz
Carrier to sideband power ratio (CSPR)	-2.2 dB
Digital filter bandwidth for carrier extraction	300 MHz
Differential phase noise compensation for QPSK	4^{th} power Viterbi-Viterbi
Differential phase noise compensation for 16- QAM	Blind phase search
Length of averaging filter	9 symbols
Total transmitted symbols for BER estimation	689655

modulates a measured complex optical field of comb lines with Nyquist pulse shaped DSCM data according to the following set of equations [20].

$$S_I(t) = \sum_{k=1}^{m} [Q_{kL}(t) - Q_{kU}(t)] \cos\left(\frac{2\pi \Delta fk}{2}\right) + \sum_{k=1}^{m} [I_{kU}(t) - I_{kL}(t)] \sin\left(\frac{2\pi \Delta fk}{2}\right) \quad (14)$$

$$S_Q(t) = \sum_{k=1}^{m} [I_{kL}(t) + I_{kU}(t)] \cos\left(\frac{2\pi \Delta fk}{2}\right) + \sum_{k=1}^{m} [Q_{kU}(t) + Q_{kL}(t)] \sin\left(\frac{2\pi \Delta fk}{2}\right) \quad (15)$$

Where, I_{kL}, Q_{kL} and I_{kU} and Q_{kU} are the in-phase and quadrature components of the kth subcarrier in the lower and upper sidebands of each optical carrier. The extracted comb lines are then modulated with independent I/Q modulators with slightly different nonlinear transfer functions and chirps. However, as these non-idealities are deterministic, they could be compensated efficiently using

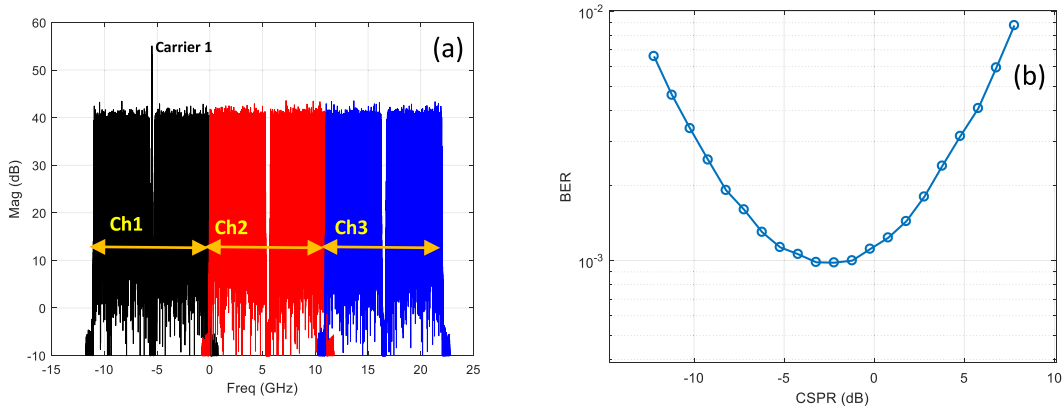

Fig. 4. (a) Superchannel arrangement. Black denotes Ch1 centered at −5.5 GHz, Red denotes Ch 2 centered at 5.5 GHz and Blue denotes Ch 3 centered at 16.5 GHz. (b) BER as a function of CSPR.

digital equalization [21]. Operating in the vicinity of two extreme wavelengths namely 1542 nm and 1548 nm allows us to investigate the impact of a large linewidth contrast on system performance.

Therefore, using the setup shown in Fig. 1(b), we obtain two complex waveforms as the local oscillator was tuned to 1542 nm and 1548 nm, respectively. The arrangement of data sidebands modulating the comb lines is shown in Fig. 4(a). Of the four comb lines reconstructed from each complex waveform (c.f. inset of Fig. 1), we consider modulating only three of them which have almost identical signal to noise ratios designated as carrier 1, carrier 2 and carrier 3.

In a practical system using a mode-locked laser with the pulse repetition rate larger than 10 GHz, a DWDM demultiplexer can be used to separate individual spectral lines for modulation, and these spectral lines are recombined in a DWDM multiplexer (wavelength interleavers may also be used to relax the requirement on DWDM devices) [8], [12]. After demultiplexing at the receiver, relative delay among comb lines may affect the phase coherence between them. For the QD-PMLL used in the experiment with the common-mode spectral linewidth $<$37MHz, if the relative delay between spectral lines within a superchannel is much less than $\sim$27ns (translates to a length mismatch of 5.4 m), this impact will not be significant. In addition, since this relative delay is deterministic, its impact can also be compensated by DSP at the receiver if necessary.

The tributaries corresponding to these three comb lines are termed as Ch1, Ch2 and Ch3, centered at −5.5 GHz, 5.5 GHz, and 16.5 GHz, respectively, and slaved to the same clock. Each tributary comprises of six 1.75 GBaud Nyquist pulse shaped DSCM subchannels, three on the upper sideband and three on the lower sideband of the comb line. Therefore, the total bandwidth occupancy by each tributary is 10.5 GHz and hence the superchannel bandwidth is 31.5 GHz. Fig. 4(a) shows that carrier component corresponding to Ch1, i.e., carrier 1 is unsuppressed. A guard band on either side of carrier 1 enables us to filter it at the receiver. However, the carrier components in Ch2 and Ch3 (i.e., carrier 2 and carrier 3) are suppressed. As a result, the Nyquist subchannels in Ch2 and Ch3 enjoy the benefit of having a better SNR compared to Nyquist subchannels in Ch1. When we use independent lasers to generate optical carriers and implement digital mixing technique at the receiver, then we ought to have a carrier unsuppressed modulation for all tributaries. On the other hand, exploiting the mutual coherence among the comb lines of a QD-PMLL, and with just one tributary having a carrier component, we can effectively eliminate common mode phase noise in at least four adjacent tributaries. (In fact, the number of tributaries benefitting from digital mixing is limited by the receiver front end bandwidth which includes devices like photodiode, transimpedance amplifier and anti-aliasing filter preceding analog to digital converter). In an actual I/Q modulator, the residual carrier component can be generated in two ways. One method is to bias the push-pull MZMs in the I/Q modulator slightly away from transmission null. Another method is to suppress the optical carrier by biasing the I/Q modulator at transmission null, and instead introduce a carrier component digitally, which after modulation has the same phase noise characteristics as

the suppressed optical carrier. Noise loading for obtaining BER waterfall curves is achieved by adding Additive White Gaussian Noise (AWGN) to the modulated signal. Differential encoding and decoding is employed to prevent cycle slips-initiated error bursts.

As mentioned in the introduction, carrier to sideband power ratio CSPR is a free parameter that can be optimized for achieving the best bit error performance. This is because, at low CSPR, the carrier component does not have high enough SNR to remove the common mode fluctuations. On the other hand, a large CSPR would take away energy from the signal sidebands making the system more susceptible to the optical noise. Our simulation results shown in Fig. 4(b) indicates that there exists an optimum CSPR of approximately -2.2 dB. This also implies that the SNR penalty incurred by each of the Nyquist subchannels in Ch1 is approximately 0.4 dB. Practically when the super-channel is transmitted through a fiber system with transmission impairments, digital compensation schemes in the receiver remain essentially the same as used in conventional coherent systems. Chromatic dispersion and PMD can be compensated using techniques such as frequency domain equalization and adaptive filtering [22], [23]. The presence of fiber nonlinearity can also be compensated using multichannel digital backpropagation [24]. It is important to note that, fiber chromatic dispersion will cause phase delay among the optical subcarriers. If uncompensated, dispersion may alter the mutual phase coherence among the comb lines within a superchannel. Therefore, by performing digital dispersion compensation before digital mixing, the dispersion-induced relative walk off can be compensated, and the phase relationship among the subcarriers is restored. On the other hand, with digital dispersion compensation, equalization enhanced phase noise (EEPN) [25] may be introduced. The finite linewidth from the local oscillator results in EEPN, whose impact on the superchannel transmission with digital mixing is similar to a system employing conventional phase noise compensation techniques. However, it is interesting to note that, as we adopt digital subcarrier multiplexing for each tributary of the superchannel, the variance of EEPN which is proportional to the baud rate is expected to decrease compared to single carrier superchannels [26].

In the process of implementing digital mixing at the receiver, we use an ideal local oscillator with zero linewidth, tuned to the frequency of carrier 1, and an ideal ADC without quantization and bandwidth limitation. However, to practically realize the simulated superchannel transmission with digital mixing, full band detection needs to be used with at least 16.5 GHz anti-aliasing filter bandwidth for the ADC. A Hann window based FIR filter with a bandwidth of 300 MHz isolates carrier 1. (We also observed that, using an ideal rectangular filter would do the job but on the flip side enhances the high frequency phase noise due to the sharp roll-off of its frequency response in the transition band). This particular bandwidth is chosen to accommodate the broad spectral linewidth of the comb line and to capture the entire common mode phase noise. In principle, a wider filter bandwidth would not only capture the comb line but also allow more broadband noise and the tail portions of the data sidebands to be included, leading to a BER performance degradation. On the other hand, a narrower filter bandwidth would not capture the tail portion of the comb line spectrum, resulting in an incomplete removal of common mode phase noise after digital mixing. Once carrier 1 is extracted by digital filtering, its complex conjugate, now used as the phase reference, is mixed with the entire signal in the time domain. This eliminates the common mode phase noise in the modulated comb lines carrier1, carrier 2 and carrier 3. After digital mixing, the desired data sideband is translated to the baseband and is demultiplexed using a matched Nyquist filter. As a part of receiver side DSP, we process the data in Ch1 differently from Ch2 and Ch3. For a Nyquist subchannel in Ch1, after frequency translation and matched filtering, we directly demodulate the data and evaluate bit errors, without any further digital phase noise compensation (DPC). On the other hand, for Nyquist subchannels in Ch2 and Ch3, we employ DPC before demodulation. Specifically, for QPSK modulation, we adopt the standard 4th power Viterbi-Viterbi algorithm and for 16-QAM, we adopt the blind phase noise compensation. The necessity of DPC arises because, carrier 2 and carrier 3 have a differential linewidth of approximately 5 KHz and 19 KHz respectively with respect to carrier1. To accommodate worst case scenario, of all the six Nyquist subchannels in a given tributary, we process and evaluate BER of the center subchannel on one side of the

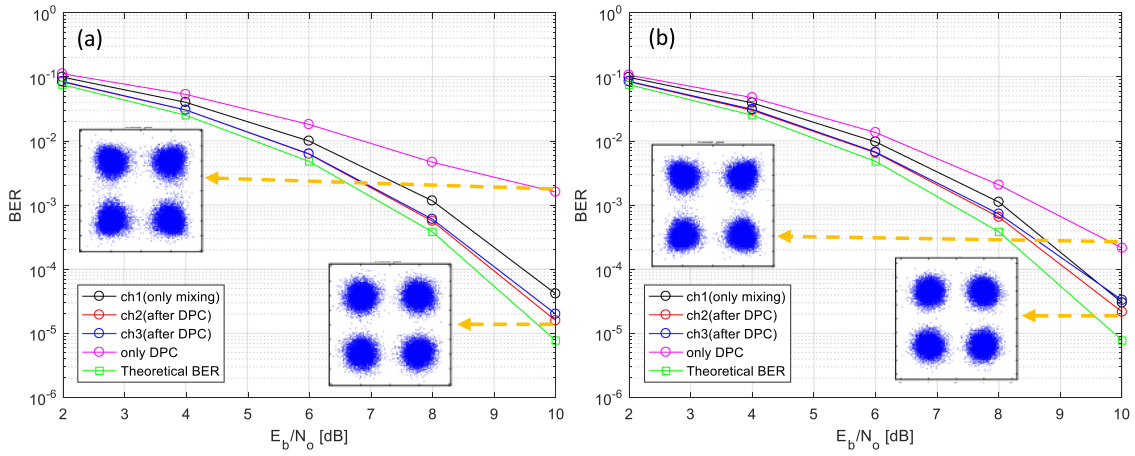

Fig. 5. QPSK modulation BER plots. (a) 1542 nm (37 MHz linewidth), (b) 1548 nm (10 MHz Linewidth). Magenta: DPC using blind phase search, Black: Ch1, Red: Ch2, Blue: Ch3, Green: theoretical differential BER. Insets depict the constellation plots.

optical carrier, which has intra-channel crosstalk from both adjacent subchannels. The total number of symbols used in BER evaluation is 689655.

Fig. 5 shows the BER plots as a function of bit energy to noise power spectral density ratio [27] (E_b/N_0) for QPSK modulated Nyquist subchannels in 1542 nm and 1548 nm regime. The black curve indicates the BER of a Nyquist subchannel from Ch1. The blue and red curves indicate BER of Nyquist subchannels from Ch2 and Ch3 respectively. The magenta curve indicates the BER obtained when using only DPC for Nyquist subchannel from Ch2 (in this case it is the 4th Viterbi-Viterbi algorithm with an averaging filter length of 9 symbols). In comparison to 4th power Viterbi-Viterbi algorithm, digital mixing reduces the required E_b/N_0 by more than 2 dB for all the Nyquist subchannels in the 1542 nm regime. With a relatively large linewidth symbol-time product, 4th power Viterbi-Viterbi algorithm is unable to track fast fluctuations of carrier phase noise irrespective of the filter length, and hence a BER of 10^{-3} cannot be achieved even at high E_b/N_0 as shown in Fig. 5(a). This indicates that digital mixing is able to effectively eliminate the common mode phase noise and performs better than the 4th power Viterbi-Viterbi algorithm especially when the optical carrier has broader spectral linewidth such as the case of QD-PMLL.

We observe that Ch2 and Ch3 have a slightly better BER performance compared to Ch1 which is attributed to carrier suppressed modulation. However, with respect to Fig. 5(b), we see that the performance enhancement brought by digital mixing in comparison to 4th power Viterbi-Viterbi algorithm is reduced because of narrow linewidth of the comb lines in 1548 nm regime. Hence, the benefit of digital mixing is more pronounced in the 1542 nm regime which has a broad linewidth compared to the 1548 nm regime. Note that, in the above numerical simulations we have not optimized the averaging filter length for every possible combination of E_b/N_0 and linewidth symbol time product. Fig. 6 provides the BER plots in the context of 16-QAM modulation. The color codes in the above plots are identical to those mentioned in QPSK BER plots. We observe that simply adopting DPC with blind phase search algorithm that includes 32 test phases and an averaging filter length of 9 symbols, will not help in estimating and compensating the phase noise, as the linewidth symbol time product is about 0.0183 [9]. It is in this scenario that digital mixing is most effective to enhance the BER performance and in fact is the only solution that produces a BER less than 10^{-3}. As a benchmark, Figs. 5 and 6 also depict the theoretical BER curves (green) with differential encoding and carrier suppressed modulation [28] obtained using the following expressions.

For QPSK,

$$P_b = 2Q\left(\sqrt{\frac{2E_b}{N_0}}\right) \tag{16}$$

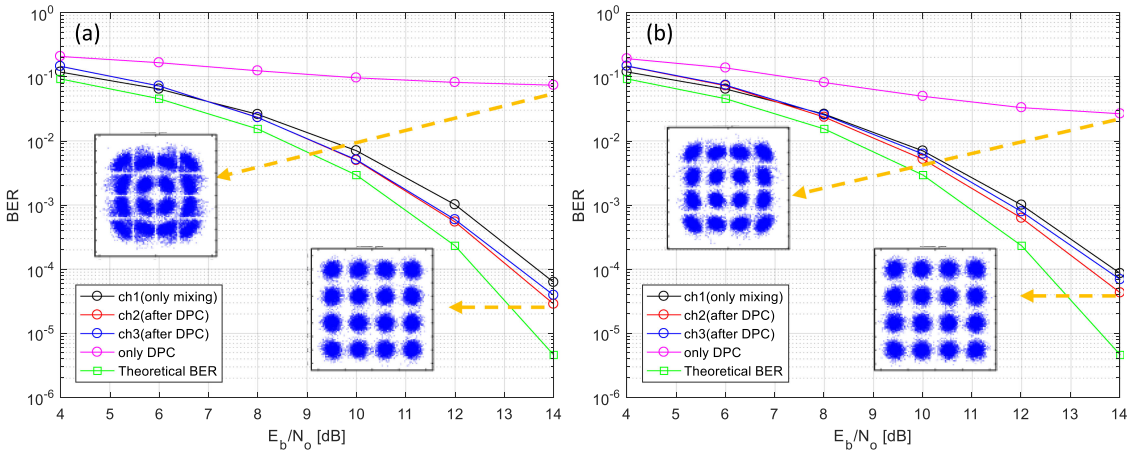

Fig. 6. 16-QAM modulation BER plots. (a) 1542 nm (37 MHz linewidth), (b) 1548 nm (10 MHz Linewidth). Magenta: DPC using blind phase search, Black: Ch1, Red: Ch2, Blue: Ch3, Green: theoretical differential BER. Insets depict the constellation plots.

For 16- QAM

$$P_b = 1.67\left(\frac{3}{4}Q\left(\sqrt{\frac{4E_b}{5N_0}}\right) - \frac{9}{16}Q^2\left(\sqrt{\frac{4E_b}{5N_0}}\right)\right) \tag{17}$$

We also noticed that, BER curves evaluated on the Nyquist subchannels from Ch2 and Ch3 deviate in the high E_b/N_0 regime despite the small difference in their linewidths after eliminating the common mode phase noise. This is primarily because, in the process of extracting the comb waveforms using the setup shown in Fig. 1, the SNR of the carrier 3 shown in the inset is slightly degraded compared to carrier1. This SNR degradation manifests itself as enhanced high frequency phase noise, after filtering with a Hann window based FIR filter.

4. Conclusion

In this paper, we propose and demonstrate by means of measurement and simulation a simple and efficient digital mixing phase noise compensation technique for Nyquist pulse shaped DSCM transmission systems employing QD-PMLL as the transmission source. Digital mixing technique outperforms conventional feedforward carrier phase recovery algorithms such as 4^{th} power Viterbi-Viterbi for QPSK and blind phase search algorithm for 16-QAM modulation in the presence of large optical linewidth. The digital mixing method has potential to allow broader linewidth, mutually coherent spectral lines of QD-PMLL, to serve as a low-cost transmission source for optical superchannels. In this context, we also demonstrate through numerical simulations, an efficient superchannel transmission together with digital mixing at the receiver. Interestingly, only one tributary of the superchannel incurs SNR penalty due to the presence of unsuppressed carrier component, unlike the case with uncorrelated optical carriers.

Acknowledgement

The authors would like to thank NRC Canada for providing the QD mode-locked laser for this research work.

References

[1] A. D. Ellis and F. C. G. Gunning, "Spectral density enhancement using coherent WDM," *IEEE Photon. Technol. Lett.*, vol. 17, no. 2, pp. 504–506, Feb. 2005.
[2] C. Liu *et al.*, "Joint digital signal processing for superchannel coherent optical communication systems," *Opt. Exp.*, vol. 21, pp. 8342–8356, 2013.
[3] V. Ataie *et al.*, "Ultrahigh count coherent WDM channels transmission using optical parametric comb-based frequency synthesizer," *J. Lightw. Technol.*, vol. 33, no. 3, pp. 694–699, Feb. 2015.
[4] J. Li, X. Zhang, F. Tian, and L. Xi, "Theoretical and experimental study on generation of stable and high-quality multi-carrier source based on re-circulating frequency shifter used for Tb/s optical transmission," *Opt. Exp.*, vol. 19, no. 2, pp. 848–860, 2011.
[5] G. Duan *et al.*, "High performance InP-based quantum dash semiconductor mode-locked lasers for optical communications," *Bell. Labs Tech. J.*, vol. 14, no. 3, pp. 63–84, 2009.
[6] X. Yi, N. K. Fontaine, R. P. Scott, and S. J. B. Yoo, "Tb/s coherent optical OFDM systems enabled by optical frequency combs," *J. Lightw. Technol.*, vol. 28, no. 14, pp. 2054–2061, Jul. 2010.
[7] E. U. Rafailov, M. A. Cataluna, and W. Sibbett, "Mode-locked quantum-dot lasers," *Nature Photon.* vol. 1, pp. 395–401, 2007.
[8] V. Vujicic *et al.*, "Quantum dash mode-locked lasers for data centre applications," *IEEE J. Sel. Topics Quantum Electron.*, vol. 21, no. 6, pp. 53–60, Nov./Dec. 2015.
[9] T. Pfau, S. Hoffmann, and R. Noe, "Hardware-efficient coherent digital receiver concept with feedforward carrier recovery for M -QAM constellations," *J. Lightw. Technol.*, vol. 27, no. 8, pp. 989–999, Apr. 2009.
[10] E. Ip and J. M. Kahn, "Feedforward carrier recovery for coherent optical communications," *J. Lightw. Technol.*, vol. 25, no. 9, pp. 2675–2692, Sep. 2007.
[11] J. Pfeifle *et al.*, "Coherent terabit communications using a quantum-dash mode-locked laser and self-homodyne detection," in *Proc. Opt. Fiber Commun. Conf. Exhib.*, Los Angeles, CA, USA, 2015, pp. 1–3.
[12] W. Freude *et al.*, "Phase-noise compensated carriers from an optical frequency comb allowing terabit transmission," in *Proc. 17th Int. Conf. Transparent Opt. Netw.*, Budapest, Hungary, 2015, pp. 1–4.
[13] D. Krause, A. Awadalla, A. S. Karar, H. Sun, and K. T. Wu, "Design considerations for a digital subcarrier coherent optical modem," in *Proc. Opt. Fiber Commun. Conf. Exhib.*, Los Angeles, CA, USA, 2017, pp. 1–3.
[14] R. Dar and P. J. Winzer, "Digital subcarrier multiplexing in optically routed networks," in *Proc. Opt. Fiber Commun. Conf. Exhib.*, Los Angeles, CA, USA, 2017, pp. 1–3.
[15] S. L. Jansen, I. Morita, T. C. W. Schenk, N. Takeda, and H. Tanaka, "Coherent optical 25.8-Gb/s OFDM transmission over 4160-km SSMF," *J. Lightw. Technol.*, vol. 26, no. 1, pp. 6–15, Jan. 2008.
[16] G. Vedala, M. Al-Qadi, M. O'Sullivan, J. Cartledge, and R. Hui, "Phase noise characterization of a QD-based diode laser frequency comb," *Opt. Exp.*, vol. 25, pp. 15890–15904, 2017.
[17] S. Chandrasekhar and X. Liu, "OFDM based superchannel transmission technology," *J. Lightw. Technol.*, vol. 30, no. 24, pp. 3816–3823, Dec. 2012.
[18] D. S. Ly-Gagnon, S. Tsukamoto, K. Katoh, and K. Kikuchi, "Coherent detection of optical quadrature phase-shift keying signals with carrier phase estimation," *J. Lightw. Technol.*, vol. 24, no. 1, pp. 12–21, Jan. 2006.
[19] L. Drzewietzki, S. Breuer, and W. Elsäßer, "Timing jitter reduction of passively mode-locked semiconductor lasers by self- and external-injection: Numerical description and experiments," *Opt. Exp.*, vol. 21, pp. 16142–16161, 2013.
[20] Y. Zhang, M. O'Sullivan, and R. Hui, "Digital subcarrier multiplexing for flexible spectral allocation in optical transport network," *Opt. Exp.*, vol. 19, pp. 21880–21889, 2011.
[21] D. J. Fernandes Barros and J. M. Kahn, "Optical modulator optimization for orthogonal frequency-division multiplexing," *J. Lightw. Technol.*, vol. 27, no. 13, pp. 2370–2378, Jul. 2009.
[22] Seb J. Savory, "Digital filters for coherent optical receivers," *Opt. Exp.*, vol. 16, pp. 804–817, 2008.
[23] T. Xu *et al.*, "Friberg, and yimo zhang, "Chromatic dispersion compensation in coherent transmission system using digital filters," *Opt. Exp.*, vol. 18, pp. 16243–16257, 2010.
[24] R Maher *et al.*, "Spectrally shaped DP-16QAM super-channel transmission with multi-channel digital back-propagation," *Sci. Rep.*, vol. 5, Feb. 2015, Art. no. 08214.
[25] T Xu *et al.*, "Equalization enhanced phase noise in Nyquist-spaced superchannel transmission systems using multi-channel digital back-propagation," *Sci. Rep.*, vol. 5, Sep. 2015, Art. 13990.
[26] M. Qiu, Q. Zhuge, M. Chagnon, F. Zhang, and D. V. Plant, "Laser phase noise effects and joint carrier phase recovery in coherent optical transmissions with digital subcarrier multiplexing," *IEEE Photon. J.*, vol. 9, no. 1, Feb. 2017, Art. no. 7901013.
[27] U. Madhow, *Fundamentals of Digital Communication*. New York, NY, USA: Cambridge Univ. Press, 2008.
[28] W. Weber, "Differential encoding for multiple amplitude and phase shift keying systems," *IEEE Trans. Commun.*, vol. COM-26, no. 3, pp. 385–391, Mar. 1978.